

Vortex Lattice in a Rotating Holographic Superfluid

Chuan-Yin Xia^{1,2}, Hua-Bi Zeng^{1,*}, Hai-Qing Zhang^{3,†}, Zhang-Yu Nie², Yu Tian^{4,1}, and Xin Li⁴

¹ *Center for Gravitation and Cosmology, College of Physical Science and Technology, Yangzhou University, Yangzhou 225009, China*

² *School of Science, Kunming University of Science and Technology, Kunming 650500, China*

³ *Center for Gravitational Physics, Department of Space Science & International Research Institute for Multidisciplinary Science, Beihang University, Beijing 100191, China and*

⁴ *School of Physical Sciences, University of Chinese Academy of Sciences, Beijing 100049, China & Institute of Theoretical Physics, Chinese Academy of Sciences, Beijing 100190, China*

By utilizing the AdS/CFT correspondence, we explore the dynamics of strongly coupled superfluid vortices in a disk with a constant angular velocity. Each vortex in the vortex lattice is quantized with vorticity one from direct inspection of its phase. As the angular velocity of the disk is greater than a critical value, the first vortex will be excited as expected from Landau's theory. The subsequent two and more vortices are also generated by increasingly rotating the disk, resulting in the remarkable steps of the angular velocities to excite each vortex. When the angular velocity is large enough, the density of the vortices is found to be linearly proportional to the angular velocity, which matches the Feynman relation very well.

Introduction.— Quantized vortex has a profound effect on the behavior of Type-II superconductors and superfluids. The quantized circulation is a macroscopic quantum mechanical effect, which is a direct consequence of a single-valued wave function, where the phase must change by $2\pi n$ ($n \in \mathbb{Z}$ is the vorticity) around a vortex core. Theoretical studies in equilibrium states predicted that the vortex lines would form a stable triangle lattice minimizing the free energy in both superconductor [1] and superfluid [2]. In experiments, vortex lines has been observed in both helium II in rotating containers [3, 4] as well as Bose-Einstein condensation (BEC) in cold atom [5, 6]. The vortex lattice formation and vortex phase diagram under a constant rotation of a container can be simulated by solving the powerful Gross-Pitaevskii equation numerically [7–10].

The AdS/CFT (Anti-de Sitter/Conformal Field Theory) correspondence [11–13] provides a novel method to explore a strongly coupled quantum system by studying the dual weakly coupled gravitational theory in a higher dimension. The holographic study of superfluid/superconductor was originally introduced in [14–16], where the $U(1)$ gauge symmetry is spontaneously broken in a AdS planar black hole background. Later, the one vortex solutions of this holographic model were obtained in both superfluid and superconductor in [17–19]. Triangle lattice solution of vortex lattice were found from perturbative calculations near critical point in [20]. In order to explore the configurations and long time dynamics of the vortex lattices, especially when the temperature is away from T_c , we need to solve the time dependent equations numerically [21].

In this letter, we will study the formation of the vortex lattices in the holographic superfluid in a constantly

rotating disk with angular velocity Ω . The quantized vortices were found by direct inspection of the phases of scalar field. We also get the quantized steps of the critical angular velocities Ω_c 's which will excite each vortex as the angular velocity is relatively small. As Ω is large enough, the density of the vortices is found to be linearly proportional to the angular velocity, which is consistent with Feynman's theoretical predictions.

Model.— A simple action for the holographic second order phase transition with $U(1)$ symmetry breaking is of a complex scalar field Ψ with mass m , minimally coupled to a $U(1)$ gauge field A_μ ,

$$S = \frac{1}{2\kappa^2} \int d^4x \sqrt{-g} \left[-\frac{F^2}{4} - |D\Psi|^2 - m^2|\Psi|^2 \right], \quad (1)$$

where $F_{\mu\nu} = \partial_\mu A_\nu - \partial_\nu A_\mu$, $D_\mu = \partial_\mu - iqA_\mu$ with q the charge. (We have set $c = \hbar = 1$.) The theory can be defined in a AdS_4 black hole background, whose metric in the Eddington-Finkelstein coordinates reads

$$ds^2 = \frac{\ell}{z^2} [-2dt dz - f(z) dt^2 + dr^2 + r^2 d\theta^2]. \quad (2)$$

in which ℓ is the AdS radius, z is the AdS radial coordinate of the bulk and $f(z) = 1 - (z/z_h)^3$. Thus, $z = 0$ is the AdS boundary while $z = z_h$ is the horizon. r and θ are respectively the radial and angular coordinates of dual 2 + 1 dimensional boundary, which is a disk in our model. For simplicity, the probe limit is adopted, by assuming that the matter fields do not affect the gravitational fields. Without loss of generality we rescale $\ell = 1$ and $z_h = 1$. Then the equation of motion are only for the matter fields Ψ and A_μ , which can be written as

$$(-D^2 + m^2)\Psi = 0, \quad d_M F^{MN} = J^N, \quad (3)$$

where $J^\mu = i(\Psi^* D^\mu \Psi - \Psi D^\mu \Psi^*)$ is the bulk electric current.

* hbzeng@yzu.edu.cn

† hqzhang@buaa.edu.cn

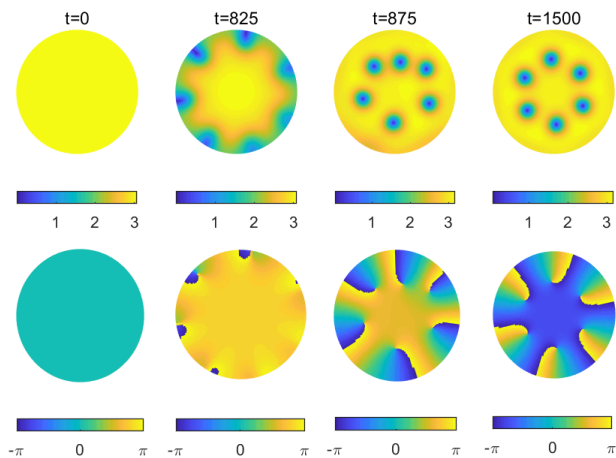


FIG. 1. Development of the superfluid vortices (top row) and their corresponding phases (bottom row) in time for $R = 5$ and $\Omega = 0.40$. Vortices enter from edge of the condensate. In the final stable state (last column with $t = 1500$), the phases of vortices vary from $-\pi$ (blue) to π (yellow), which demonstrates that the vortices are quantized with vorticity $n = 1$. The quantum vortices coincide with the singularities (branch points) in the phase visualizations.

In order to solve the equations (3), we choose the axial gauge as $A_z = 0$. These equations need to be solved with boundary conditions at the horizon and the boundary. At the horizon, physical solutions should be regular. Near the boundary, the general solution takes the asymptotic form

$$A_\nu(t, z, r, \theta) = a_\nu(t, r, \theta) + b_\nu(t, r, \theta)z, \quad (4)$$

$$\Psi(t, z, r, \theta) = \Psi^1(t, r, \theta)z + \Psi^2(t, r, \theta)z^2. \quad (5)$$

in which $a_{r,\theta}$ can be interpreted as a dynamical vector potential then the dual system is a superconductor, which corresponds to fixing the dual current $b_{r,\theta}$ to be zero at the boundary. On the contrary, the coefficients $a_{r,\theta}$ can also be considered as the superfluid velocities for a superfluid[16]. We will adopt the later interpretation in this letter, i.e., by fixing the $a_{r,\theta}$ to be a constant. Ψ^1 is an external source for the condensate Ψ^2 , which has to be zero in order to find a spontaneous symmetry breaking solution. The time component a_t is the chemical potential of the superfluid disk. In the homogeneous case where all the fields are r, θ independent, by taking a_t larger than a critic value, the bulk scalar field Ψ will condense, which is a holographic version of Higgs mechanism. In this letter we set $m^2 = -2$, thus the critical chemical potential is about $a_t \sim 4.06$. Such a homogeneous holographic superconductor/superfluid model gives insights to the dynamics of a continuous phase transition even in far from equilibrium dynamics[24–27], the nonlinear response to a strong external field[28, 29], as well as the critical behavior of a non-equilibrium phase transition[30]. Extending the equations to the cases with all coordinates dependent gives a systematic new and first-principle approach to study quantum turbulence [22, 31], and also to the topo-

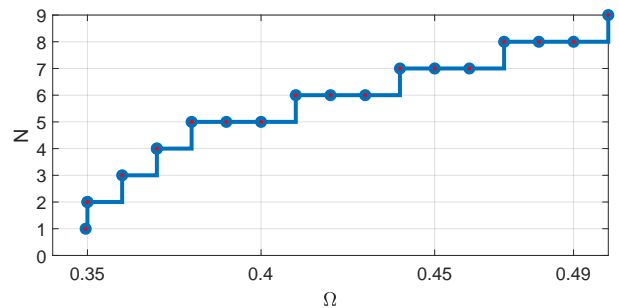


FIG. 2. Vortex number N as a step function of Ω at small frequencies. There is a critical angular velocity $\Omega_{c1} \sim 0.3498$ where the first vortex is generated. The subsequent two, three and more vortices can also be excited at higher critical angular velocities, which can be demonstrated by the step-wise relations between them.

logical defects formation predicted by the Kibble-Zurek mechanism[32, 33].

In order to study the process of vortex lattice formation in the holographic superfluid disk with a constant angular velocity, we impose the boundary condition following[23]

$$a_\theta = \Omega r^2, \quad (6)$$

where Ω is the constant angular velocity of the disk. The equations (3) are solved numerically by the Chebyshev spectral method in the z, r direction, while Fourier decomposition is adopted in the θ direction. The time evolution is simulated by the fourth order Runge-Kutta method. The initial configuration is chosen to be a homogenous superfluid state without rotation at the temperature $T = 0.82T_c$.

Quantized vortex lattice and Feynman relation— According to Landau’s two-fluids model of superfluid [36], the normal components behave like ordinary liquids while the superfluid components move without dissipation. These two components can have different velocities: v_n for the normal parts and v_s for the superfluid parts. The container (a two-dimensional disk in our case) rotates at a constant angular velocity Ω , then the normal component circulates accordingly similar to a rigid body. This motion implies that the linear velocity $v_n = \Omega r$ and the curl $\nabla \times v_n = 2\Omega$, in which r is the position vector with its origin at the vortex center. However, the superfluid remains stationary, i.e., $v_s = 0$, at small Ω , which is called the Landau state. This resembles the Meissner state that a small magnetic field cannot penetrate the superconductor. But a stationary liquid in a rotating container implies a high free energy. When Ω increases to a critical value Ω_{c1} , the Landau state becomes unstable and prefers entering a state with one vortex. Keep increasing Ω to the second critical velocity Ω_{c2} , the lowest energy state of the system renders two quantized vortices located symmetrically in the disk. Consequently, higher angular velocities will excite the third, fourth, and subsequent more vortices, which will arrange themselves in the disk according to the minimum of the free energy.

The top row of Fig.1 shows the development of the

vortex lattices (with 6 vortices) during time from $t = 0$ to final stable state $t = 1500$ for $R = 5$ and $\Omega = 0.4$. At the time $t \sim 825$ the vortices begin to form from the edge of the disk, and at later time vortices will rotate into the inner side of the disk. A stable vortex lattice forms at final $t = 1500$. The bottom row of Fig.1 plots the corresponding phases of the superfluid in top row. At the final stable time, the locations of the vortices can be seen from the singularities or branch points of the phases. Circling around the vortex core, we can see that the phases vary from $-\pi$ (blue) to π (yellow) with discrepancy 2π , which proves that each vortex is quantized with $n = 1$.

In Fig.2, we show the typical step-wise relation between N and Ω , from $N = 1$ to $N = 8$ still for the case of $R = 5$. The corresponding critical angular velocities $\Omega_{c1}, \Omega_{c2} \dots$ are obtained. By increasing the angular velocity to $\Omega_{c1} \sim 0.3498$, the first vortex is excited by the rotation of the disk [36]. The next two, three and more vortices can also be generated at some larger critical velocities. However, we see that the spacings between these critical angular velocities are not always equal, which may make confusion that the vortices do not have the same energy. This can be explained that there are still small orbital angular velocities of the vortices rotating along the axis of the disk, which will cost some energy. Indeed, from Fig.1 we see that the 6 vortices will rotate as a whole around the axis with angular velocity $\omega \sim 0.0018$. Although this angular velocity ω is small compared to the angular velocity Ω of the disk, a large number of vortices will cost more energies. Another possible reason for the unequal spacings is that the appearance of vortex will in some sense break the superfluidity of the superfluid. The normal components of the superfluid will scatter at the vortices, leading to the frictions between the normal and superfluid components inside the disk [36]. This friction will also cost some energies which may result in the unequal spacings of the critical angular velocities. Theoretical studies in condensed matter [37] also showed the unequal spacings of the critical angular velocity as vortex number is small.

The first critical angular velocity Ω_{c1} in two-dimensional superfluids can be obtained from an refined analytical calculation [38, 39] as (We have set $\hbar = 1$ as we mentioned before.)

$$\Omega_{c1} = \frac{2}{MR^2} \ln \left(\frac{0.888R}{a} \right), \quad (7)$$

where a denotes the coherence length of the scalar field without a vortex, while R is the radius of the disk and M is the atom mass of the superfluid. We estimate the coherence length a from the quasi-normal modes method of the superfluid without any vortex. At the temperature in our case, we find that $a \sim 0.60$. Therefore, we can estimate $M \sim 0.4577$.

At larger frequency $\Omega \gg \Omega_{c1}$, quantum vortices attempt to distribute as uniformly as possible. Moreover, in this case the rotations of the superfluid with a large number of vortices can be regarded as the rotation of

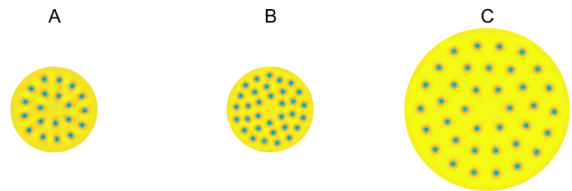


FIG. 3. Configuration of a large number of vortex lattices, with $N = 20(A), 33(B)$ and $37(C)$ corresponding to $(R, \Omega) = (11, 0.27), (11, 0.34)$ and $(21, 0.1)$, respectively. The number N agree well with the Eq.(8).

a rigid body [36]. Therefore, the vorticity equals to $\nabla \times \vec{v} = 2\Omega$. Then the circulation can be computed according to Stokes' theorem $\Gamma = \oint \vec{v} \cdot d\vec{l} = 2\Omega\pi R^2$. Since the circulation of a vortex is just the quantum number, thus the number of vortices can be easily determined from the condition that the velocity circulation along a contour enclosing a large number of vortices should correspond to the rotation of the liquid as a whole. If such a contour encloses all the vortices along the circumference of the disk, then the total number of vortices N admit the Feynman relation [40] as

$$N = \frac{M\Omega}{\pi} \pi R^2, \quad (8)$$

where $n \equiv \frac{M\Omega}{\pi}$ is the vortex number density.

In Fig.3 we show the configurations of vortex lattices with large vortex numbers $N = 20(A), 33(B)$ and $37(C)$, corresponding to $(R, \Omega) = (11, 0.27), (11, 0.34)$ and $(21, 0.1)$, respectively. These vortex lattices are uniformly distributed from the symmetry of the disk as well as the condition of the lowest free energy. From the relation Eq.(8), we may estimate the values of M from the subplots A, B and C of Fig.3. We obtain $M(A) \sim 0.6122, M(B) \sim 0.8021$ and $M(C) \sim 0.8390$ respectively. The values of M in subplot B and C are close since the Eq.(8) is valid only for large number of vortices, however, the number of vortices in subplot A is only 20 which seems not large enough. For this reason, we plot a large number of vortices with respect to Ω in the left panel of Fig.4 by fixing $R = 11$. For large number of vortices, one can fit the linear relation between N and Ω as $N \sim 103.2634\Omega$. Thus, comparing this fitting line with Eq.(8), we can readily get that $M \sim 0.8534$. Therefore, the relation Eq.(8) becomes

$$N \sim 0.8534\Omega R^2. \quad (9)$$

In the right panel of Fig.4, we show the relation between large number of vortices to the radius R of the disk by fixing the angular velocity $\Omega = 0.17$. The direct fitting of the curve in the right panel of Fig.4 is $N \sim 0.1451R^2$. By comparison, replacing $\Omega = 0.17$ into Eq.(9) we get $N \sim 0.1450R^2$, which perfectly matches the fitting from the right panel of Fig.4. Therefore, this in turn numerically demonstrates the Feynman relation Eq.(8)!

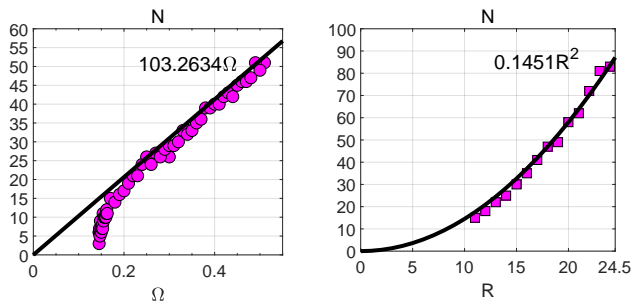


FIG. 4. Left: Compare Eq.7 to the results when the disk size is relatively small $R = 11$. Right: Compare Eq.7 to the results when the angular velocity is fixed to be $\Omega = 0.17$.

Discussions and Summaries.— There is still one thing needs to be clarified. We get $M \sim 0.8534$ from the analysis of large number of vortices, however, we also obtain $M \sim 0.4577$ from the critical angular velocity as vortex number is small enough. There are roughly two times difference of M from the analysis in opposite limit of vortex numbers. Actually the estimation of M from large number of vortices is more reliable. One reason is that as we see from above the Feynman relation fits very well from the two different estimations in Fig.4; The other reason is that in the case of large number vortices, the superfluid can be reasonably regarded as a rigid body which does not make any differences from strongly and weakly

coupled theories. It is well-known that from AdS/CFT correspondence, the boundary field is strongly coupled in the limit of large N_c and 't Hooft coupling [11–13]. Therefore, Landau's theory about the excitation of quasiparticles in rotating superfluid disk [36] cannot be applied in strongly coupled superfluid, which is indeed the holographic superfluid in our case. Thus, the relation Eq.(7) we used to estimate the value of M from the critical angular velocity is not applicable in holographic superfluid. Nevertheless, even in strongly coupled holographic superfluids one can still see the quantized vortex lattices as expected from quantum mechanics.

We give a first successful attempt to adopt the holographic methods to systematically study the vortex lattice formation in a strongly coupled superfluid in a constantly rotating disk. This gives insights to understand the properties of cold atom BEC experiments under fast rotations. The numerical results we obtained match the known experimental and theoretical conclusions. There are still many interesting topics to work in future. For instance, configurations of the vortices may receive deformations due to thermal fluctuations or inhomogeneous of the background. Thus, to develop a more powerful numerical technic to compute these fruitful patterns of the superfluid vortices is a very interesting task.

Acknowledgements.— This work is supported by the National Natural Science Foundation of China (under Grant No. 11675140, 11705005, 11875095 and 11675015). Y.T. is also supported by the “Strategic Priority Research Program of the Chinese Academy of Sciences” with Grant No.XDB23030000.

-
- [1] A. A. Abrikosov, Sov. Phys. JETP **5**, 1174 (1957).
[2] V. K. Tkachenko, Sov. Phys. JETP **22**, 1282 (1966); **23**, 1049 (1966); **29**, 945 (1969).
[3] E.J. Yarmchuk, M.J.V. Gordon and R.E. Packard, Phys. Rev. Lett. **43** 214 (1979).
[4] G.P. Bewley, D.P. Lathrop and K. R. Sreenivasan, Nature **441** 588 (2006).
[5] K. W. Madison, F. Chevy, W. Wohlleben, and J. Dalibard, Phys. Rev. Lett. **84**, 806 (2000).
[6] J. R. Abo-Shaeer, C. Raman, J. M. Vogels, and W. Ketterle, Science **292**, 476 (2001).
[7] C.J. Pethick and H. Smith, Bose-Einstein Condensation in Dilute Gases, Cambridge University Press, Cambridge (2002).
[8] A. L. Fetter, Rev. Mod. Phys. **81**, 647 (2009).
[9] K. Kasamatsu, M. Tsubota, M. Ueda, Phys. Rev. Lett. **91** 150406 (2003).
[10] K. Kasamatsu, M. Tsubota, Phys. Rev. Lett. **97**, 240404 (2006).
[11] J. M. Maldacena, Adv. Theor. Math. Phys. **2**, 231 (1998).
[12] S. S. Gubser, I. R. Klebanov, and A. M. Polyakov, Phys. Lett. B **428**, 105 (1998).
[13] E. Witten, Adv. Theor. Math. Phys. **2**, 253 (1998).
[14] S. S. Gubser, Phys. Rev. D **78**, 065034 (2008).
[15] S. A. Hartnoll, C. P. Herzog, and G. T. Horowitz, Phys. Rev. Lett. **101**, 031601 (2008).
[16] C. P. Herzog, P. K. Kovtun and D. T. Son, Phys. Rev. D **79**, 066002 (2009).
[17] M. Montull, A. Pomarol and P. J. Silva, Phys. Rev. Lett. **103**, 091601 (2009).
[18] J. C. Dias, G. T. Horowitz, N. Iqbal and J. E. Santos, JHEP **1404**, 096 (2014).
[19] M. S. Wu, S. Y. Wu and H. Q. Zhang, JHEP **1605**, 011 (2016).
[20] K. Maeda, M. Natsuume and T. Okamura, Phys. Rev. D **81**, 026002 (2010).
[21] X. Li, Y. Tian and H. Zhang, arXiv:1904.05497.
[22] A. Adams, P. M. Chesler, and H. Liu, Science **341**, 368 (2013).
[23] O. Domenech, M. Montull, A. Pomarol, A. Salvio and P. J. Silva, JHEP **1008**, 033 (2010).
[24] K. Murata, S. Kinoshita, and N. Tanahashi, JHEP **1007**, 050 (2010).
[25] M. J. Bhaseen, J. P. Gauntlett, B. D. Simons, J. Sonner, and T. Wiseman, Phys. Rev. Lett. **110**, 015301 (2013).
[26] W. J. Li, Y. Tian and H. b. Zhang, JHEP **1307**, 030 (2013).
[27] X. Bai, B. H. Lee, L. Li, J. R. Sun and H. Q. Zhang, JHEP **1504**, 066 (2015).
[28] H. B. Zeng, Y. Tian, Z. Y. Fan and C. M. Chen, Phys.

- Rev. D **93**, 121901 (2016).
- [29] H. B. Zeng, Y. Tian, Z. Fan and C. M. Chen, Phys. Rev. D **95**, 046014 (2017).
- [30] H. B. Zeng and H. Q. Zhang, Phys. Rev. D **98**, no. 10, 106024 (2018).
- [31] Y. Du, C. Niu, Y. Tian and H. Zhang, JHEP **1512**, 018 (2015).
- [32] P. M. Chesler, A. M. Garcia-Garcia and H. Liu, Phys. Rev. X **5**, no. 2, 021015 (2015).
- [33] J. Sonner, A. del Campo and W. H. Zurek, Nature Commun. **6**, 7406 (2015)
- [34] L. J. Campbell, R. M. Ziff, Phys. Rev. B **20**, 1886 (1979).
- [35] Y. Castin, R. Dum, Eur. Phys. J. D **7**, 399 (1999).
- [36] L.D.Landau and E.M.Lifshitz, Statistical Physics, Part 2,(Oxford: Pergamon,1981).
- [37] G. B. Hess, Phys. Rev., **161**, 189, (1967).
- [38] P. Nozières and D. Pines, The Theory of Quantum Liquids (Addison-Wesley, Reading, MA, 1990).
- [39] E. Lundh, C. J. Pethick, H. Smith, Phys. Rev. A **55**, 2126 (1997).
- [40] R. P. Feynman, Progress in Low Temperature Physics, **1**,17-53, (1955).